

## Suppression of Thermal Effects in Femtosecond Laser Processing of Fiber Bragg Gratings \*

CUI Wei(崔巍), SI Jin-Hai(司金海), CHEN Tao(陈涛)\*\*, YAN Fei(严飞), CHEN Feng(陈烽), HOU Xun(侯洵)

Key Laboratory for Physical Electronics and Devices of the Ministry of Education & Shaanxi Key Lab of Information Photonic Technique, School of Electronics & Information Engineering, Xi'an Jiaotong University, Xi'an 710049

(Received 18 June 2013)

*Thermal effects on the processing of type-I IR fiber Bragg gratings (FBGs) using a femtosecond laser with phase mask are investigated. Thermal effects are significantly suppressed by using interval exposure mode and reducing the tension on the fiber. FBGs with improved photo-induced refractive index modulation are fabricated in the standard telecom fiber. The index modulation reaches  $1.6 \times 10^{-3}$ . The reflectivity and bandwidth are measured to be  $-0.36$  dB and  $1.27$  nm, respectively.*

PACS: 42.79.Dj, 42.81.Bm, 42.62.Cf

DOI: 10.1088/0256-307X/30/10/104207

Fiber Bragg gratings (FBGs) have been broadly applied in the field of optical fiber sensors. Due to their excellent sensing characteristics, they are suitable for temperature, strain and refractive index measurements.<sup>[1,2]</sup> Their unique filtering properties also make them important components in communication devices such as phase conjugators, wavelength converters, wavelength division multiplexers, and optical switch.<sup>[3-5]</sup> FBGs are promising to apply to all-optical router and optical buffers owing to their tunable group velocity.<sup>[6]</sup>

The conventional method to fabricate FBGs is using an ultraviolet (UV) excimer laser to write gratings in fibers. It requires the fibers to be photosensitive or hydrogen loaded.<sup>[7]</sup> In recent years, femtosecond infrared (IR) laser systems have been proved to be useful for processing FBGs.<sup>[8]</sup> Unlike the UV method, femtosecond laser processing can be used to fabricate FBGs in various optical fibers which are not photosensitive,<sup>[9]</sup> due to its high peak power intensities and the strong nonlinear interaction between light and materials.<sup>[10]</sup> In addition, FBGs fabricated with femtosecond IR laser exhibit higher thermal stability than regular gratings, making them suitable for sensing applications in harsh environments such as monitoring furnaces, combustion situations, etc.<sup>[11]</sup> When combined with the phase mask technique, it gives a highly repeatable spatially modulated interference field and ease of alignment.

There are two intensity-dependent regimes of ultrafast IR induced refractive index modulation in the fiber.<sup>[12]</sup> Above the threshold intensity of multiphoton ionization (MPI), localized melting or void formation that results from dielectric breakdown is the primary cause of index modulation. This is referred to as type-II IR index modulation. Below the threshold intensity,

multiphoton absorption that results in defect formation causes the index changes. This is referred to as type-I IR index modulation.<sup>[13]</sup> However, when a femtosecond laser with high repetition rate is used in the processing of the type-I IR gratings, heat accumulation in the material is considerable.<sup>[14]</sup> The thermal effects will have significant influence on the formation of grating fringes and the ac part of index modulation  $\Delta n$ , which results in an unsatisfactory optical quality.

In this Letter, we investigate the thermal effects in the femtosecond laser processing of FBGs. By using interval exposure mode and reducing the tension on the fiber, we minimize the negative influence. FBGs with improved photo-induced index modulation are fabricated in a standard telecom fiber (SMF-28). The reflectivity and bandwidth are measured to be  $-0.36$  dB and  $1.27$  nm, respectively.

Femtosecond laser pulses with 150-fs duration were generated by an amplified Ti:sapphire laser at a central wavelength of 800 nm and 1-kHz repetition rate. The laser has maximum output energy of about 1.2 mJ. The 12 mm diameter Gaussian beam was focused with a 50 mm cylindrical lens through a zero-order nulled phase mask with a period  $\Lambda_m = 2.14$   $\mu$ m into the SMF-28 fiber core. The pitch of the fabricated FBG is  $\Lambda_G = \Lambda_m/2 = 1.07$   $\mu$ m. Due to the relation  $m\lambda = 2n_{\text{eff}}\Lambda_G$ , in which  $m$  is the order number and  $n_{\text{eff}}$  is the effective index of the fiber, the second-order Bragg resonance occurs at  $\lambda = 1550$  nm.

To obtain pure two-beam interference gratings with a femtosecond pulse, the distance between fiber and phase mask was set to  $\sim 3$  mm. Thus the diffracted beams of different order pairs (0,  $\pm 1$ ,  $\pm 2$ , etc.) would not overlap spatially resulting from an order walk-off effect.<sup>[15]</sup> Under this setup the length of interference field was calculated to be  $\sim 7.5$  mm, which was long

\*Supported by the National Basic Research Program of China under Grant No 2012CB921804, the National Natural Science Foundation of China under Grant Nos 11204236 and 91123028.

\*\*Corresponding author. Email: tchen@mail.xjtu.edu.cn

© 2013 Chinese Physical Society and IOP Publishing Ltd

enough for the fabrication. According to free space Gaussian beam optics, the Rayleigh length for the focused beam is  $z_R = \pi\omega^2/\lambda = 17.3\ \mu\text{m}$ . The width of the focal spot size is  $W = 2\omega \approx 2\lambda f/\pi\omega_0$ , where  $\lambda$  is the wavelength,  $f$  is the focal length of the cylindrical lens, and  $\omega_0$  is the incident beam waist. Thus the focus area is  $4.2\ \mu\text{m} \times 10\ \text{mm}$ . For  $700\ \mu\text{J}$  pulse energy, the peak intensity in the focus area was estimated to be  $2 \times 10^{13}\ \text{W}/\text{cm}^2$ , which was smaller than the threshold intensity for multi-photon ionization. Thus the FBGs we fabricated belong to type-I IR gratings.

First, we fabricated FBGs using continuous exposure. Figure 1 shows the reflectivity and bandwidth of FBGs as a function of exposure time using continuous exposure. The pulse energy was set to  $700\ \mu\text{J}$ . Exposure time was set to 5, 10, 20, 30, 60 and 90 s, respectively. We can see that the maximum reflectivity and bandwidth were about  $-1.95\ \text{dB}$  and  $0.29\ \text{nm}$ , respectively, and then both of them decreased with exposure time increasing from 10 s. The descending of reflectivity and bandwidth would be quicker when we increased the pulse energy. This indicated that  $\Delta n$  could not increase monotonically with the increase of the exposure time when we used continuous exposure. The maximum  $\Delta n$  was determined to be  $3 \times 10^{-4}$ . The length of gratings was measured to be  $< 2.7\ \text{mm}$  using an optical microscope. Due to the relation  $R_{\text{max}} = \tanh^2(\kappa L)$ , it also has influence on the reflectivity.

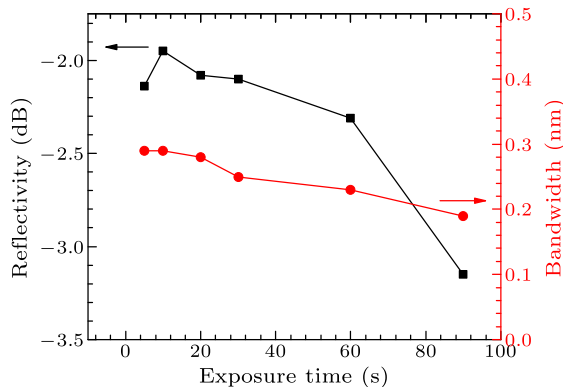


**Fig. 1.** Reflectivity (square) and bandwidth (circle) of FBGs as a function of exposure time using continuous exposure.

Then we took the thermal effects on the grating formation into account. The temperature of exposure area in the fiber would rise when writing gratings. Then the fiber would expand. The fiber was tensed when fixed on the translation stage to make sure it straight and stable enough for focusing alignment. With temperature rising, the elastic modulus of fiber would decrease. Both effects would lead to the elongation of fiber. Since the grating period was only  $1.07\ \mu\text{m}$ , the elongation would break the overlap between the grating fringes that had already formed

and the interference pattern. Therefore, the further exposure would increase the refractive index of the area between the grating fringes, which results in the decrease of the  $\Delta n$ . This mismatch problem would be more considerable in the side area as the shifting was larger here. The influence of tension is related to the decrease of elastic modulus caused by the thermal loading. The thermal loading also leads to the expansion of fiber directly. Thus reducing the thermal loading of fiber under exposure plays a key role in the processing.

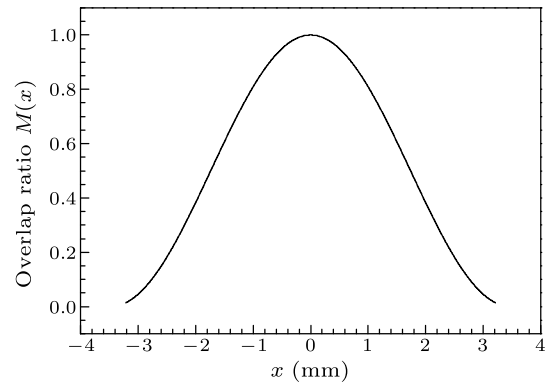


**Fig. 2.** The overlap ratio of the interference fringes and photoinduced gratings taking the thermal effects into account.

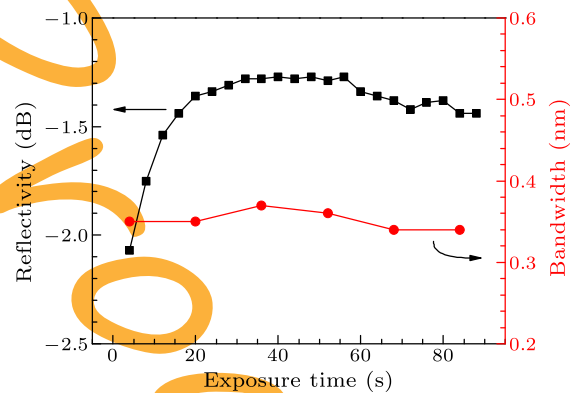


**Fig. 3.** Reflectivity (square) and bandwidth (circle) of FBG as a function of exposure time using interval exposure.

Here we assume that the laser beam is uniform, and the intensity modulation profile of interference field can be expressed as  $P(x) = \cos(2\pi x/\Lambda_G)$ , where  $x$ -axis is oriented along the fiber direction, and the FBG center is taken as zero. Under irradiation of laser, the elongated grating modulation profile can be expressed as  $G(x) = \cos[2\pi x/(1 + \Delta T\alpha)\Lambda_G]$ , in which the  $\Delta T$  is the increase of fiber temperature, and the  $\alpha$  is the thermal expansion coefficient ( $5.5 \times 10^{-7}$  for silica). The overlap ratio of the interference fringes and photo-induced gratings can be indicated by the following equation:

$$M(x) = 1 - |P(x) - G(x)|/2. \quad (1)$$

We only need to calculate the value of  $M(x)$  at each interference peak position, where  $P(x) = 1$ , to indicate the overlap ratio. The results calculated for the overlap ratio  $M(x)$  are plotted in Fig. 2, in which we assume that the temperature of fiber increased by 300°C under the continuous exposure. From Fig. 2, we can see that  $M(x)$  is approximate 1 near the FBG center, indicating the interference fringes and the grating stripes overlap perfectly. At both edges of the FBG, the overlap ratio of the interference fringes and photo-induced gratings decreases to its minimum value.

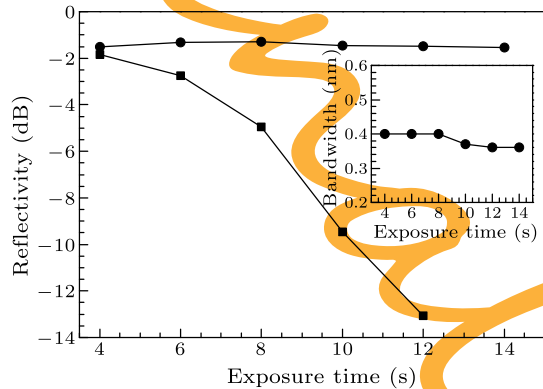


**Fig. 4.** Reflectivity of FBGs as a function of exposure time under larger (square) tension and minimized (circle) tension. The inset shows the bandwidth of FBG as a function of exposure time under minimized tension.

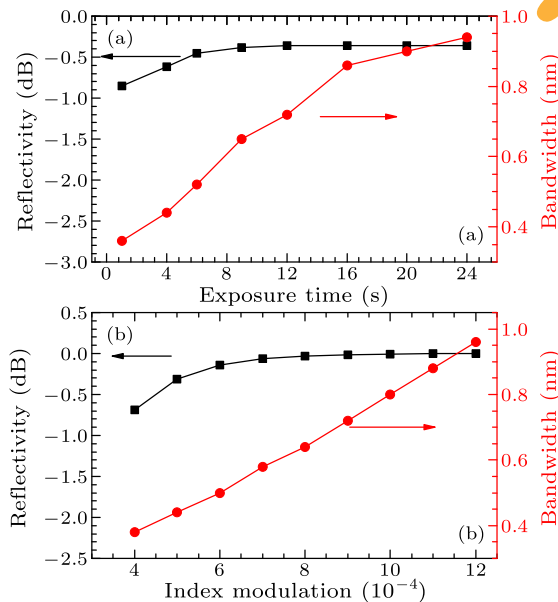


**Fig. 5.** (a) Reflectivity (square) and bandwidth (circle) of FBGs with both the exposure and tension optimized as a function of exposure time. (b) Simulated reflectivity (square) and bandwidth (circle) of a 5-mm-long Gaussian-apodized FBG as a function of  $\Delta n$ .

To avoid thermal loading, we adopted the interval exposure and reduced the time of every single exposure. The pulse energy was set to 700  $\mu\text{J}$ . The exposure time was set to 4 s and interval time was set

to 60 s. The interval time was long enough to eliminate the heat accumulation in the fiber. The reflection spectra were recorded between each exposure. Figure 3 shows reflectivity and bandwidth of FBG fabricated using interval exposure as a function of exposure time. The reflectivity of the FBG reached  $-1.27$  dB after 40 s exposure, and decreased very slowly with the increase of the exposure times. After 88 s total exposure the reflectivity of the FBG fabricated using interval exposure setups was  $-1.44$  dB, which is still better than the FBG fabricated using continuous exposure. The bandwidth stayed around 0.35 nm and did not increase sustainably with the increase of the exposure time as shown in Fig. 3. The results demonstrated that the thermal effects that caused the decrease of  $\Delta n$  were partly restrained.

Because the tension on the fiber will enhance the elongation along the fiber, we compared the reflectivity of two sets of FBGs fabricated at different tensions, in which the same interval exposure was used. One had larger tension on it, and the other one had minimized tension by using a modified fiber holder. The pulse energy was set to 700  $\mu\text{J}$ . The exposure time for both groups was 2 s, and the interval time was 60 s. Figure 4 shows the reflectivity of FBGs as a function of exposure time. The reflectivity of FBGs fabricated with larger tension decreases from  $-1.83$  dB to  $-13.06$  dB in 12 s. While the reflectivity of FBG fabricated with minimized tension reached the maximum value of  $-1.33$  dB in 6 s and decreased slowly to  $-1.53$  dB after 14 s exposure. However, the bandwidth of FBG fabricated under minimized tension still did not increase sustainably with the increase of the exposure time as shown in the inset of Fig. 4. The results demonstrated that the tension had influence on the processing of FBG.

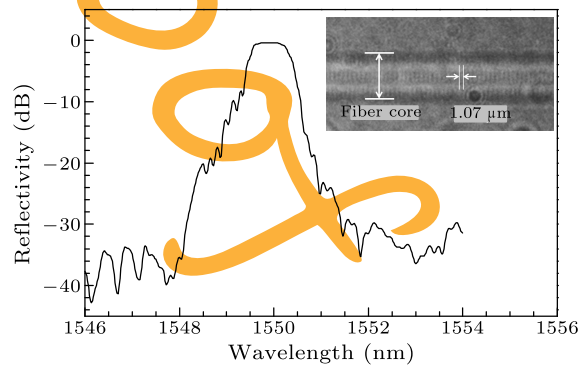


**Fig. 6.** Reflection spectra of the FBG after 24 s exposure. Inset is optical microscope images of the grating structure in SMF-28 with 1.07  $\mu\text{m}$  grating period.

In order to suppress thermal effects in the processing, the exposure time was reduced to 0.2 s, and the interval time was set to 10 s, which is the optimized exposure setting up. The fiber was fixed on the modified holder with minimized tension. Figure 5(a)

shows reflectivity and bandwidth of FBGs fabricated at the optimized condition as a function of exposure time. From Fig. 5(a), we can see that the reflectivity reaches its maximum value,  $-0.36$  dB after 12 s exposure, which was mainly attributed to the transmission loss of our detection system. Further exposure would not cause the decrease of reflectivity. From Fig. 5(a), we can also see that the bandwidth keeps increasing when the exposure time is increased. The results demonstrated that the index modulation had not saturated as yet, and the growth of index modulation was sustainable. The index modulation would be saturated by increasing the exposure time or the pulse energy. The trends of reflectivity and bandwidth agree well with the simulation results of a 5-mm-long Gaussian-apodized FBG as shown in Fig. 5(b).

Reflection spectra of the FBG fabricated after 24 s exposure is shown in Fig. 6, having a flat top shape. The bandwidth was measured to be  $0.94$  nm. The inset of Fig. 6 shows the photograph of the FBG observed using an optical microscope, and the grating structure with a period of  $1.07$   $\mu\text{m}$  can be observed. The length of FBGs was measured to be over  $4.7$  mm, which is much longer than before. With the help of commercial software, the index modulation corresponding to the bandwidth was  $1.2 \times 10^{-3}$ .

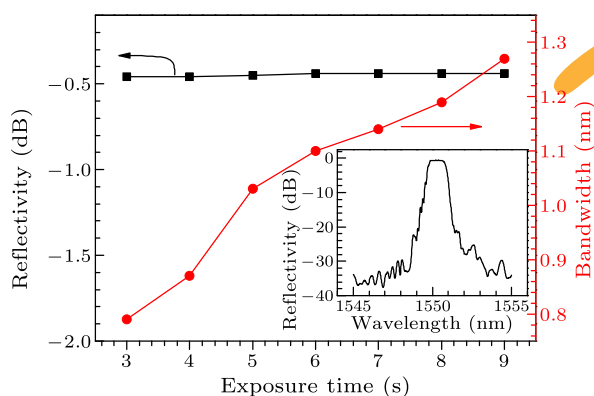


**Fig. 7.** The reflectivity (square) and bandwidth (circle) of FBG written with  $870$   $\mu\text{J}$  pulse energy as a function of exposure time. The inset shows the reflection spectra after 9 s total exposure.

This method allows us to use higher pulse energy in the processing, because the thermal effects could be suppressed effectively. We used the optimized exposure setting up and set the pulse energy to  $870$   $\mu\text{J}$ .

Figure 7 shows the reflectivity and bandwidth of the fabricated FBGs as a function of exposure time. From Fig. 7 we can see that the reflectivity of FBG stabilizes at  $-0.44$  dB after 6 s. The actual reflectivity should be higher if taking the insertion loss of fiber connectors into consideration. The bandwidth increases to  $1.27$  nm continuously with the increase of exposure time. The bandwidth of  $1.27$  nm indicates an index modulation of about  $1.6 \times 10^{-3}$  was induced.

In conclusion, we have presented a method using interval exposure mode and reducing the tension on the fiber to suppress the thermal effects in the femtosecond laser processing of FBGs. FBGs with improved photo-induced index modulation have been fabricated in fibers. The reflectivity and bandwidth were measured to be  $-0.36$  dB and  $1.27$  nm, respectively. The experimental results show that thermal effects can be suppressed using this interval exposure mode although it will take longer time to produce FBG with high reflectivity. The method can be applied to improve the processing quality of FBGs in fibers susceptible to the thermal effects.

## References

- [1] Rao Y 1999 *Meas. Sci. Technol.* **8** 355
- [2] Liang R B, Sun Q Z, Wo J H and Liu D M 2011 *Acta Phys. Sin.* **60** 104221 (in Chinese)
- [3] Giles C R 1997 *J. Lightwave Technol.* **15** 1391
- [4] Ouellette F, Krug P A, Stephens T, Dhosi G and Eggleton B 1995 *Electron. Lett.* **31** 899
- [5] Kabakova I V, Grobncic D, Mihailov S, Mägi E C, de Sterke C M and Eggleton B J 2011 *Opt. Express* **19** 5868
- [6] Shahoei H, Li M and Yao J 2011 *J. Lightwave Technol.* **29** 1465
- [7] Lemaire P J, Atkins R M, Mizrahi V and Reed W A 1993 *Electron. Lett.* **29** 1191
- [8] Martinez A, Dubov M, Khrushchev I and Bennion I 2004 *Electron. Lett.* **40** 1170
- [9] Mihailov S J, Smelser C W, Lu P, Walker R B, Grobncic D, Ding H, Henderson G and Unruh J 2003 *Opt. Lett.* **28** 995
- [10] Davis K M, Miura K, Sugimoto N and Hirao K 1996 *Opt. Lett.* **21** 1729
- [11] Mihailov S J, Grobncic D, Smelser C W, Lu P, Walker R B and Ding H 2011 *Opt. Mater. Express* **1** 754
- [12] Sudrie L, Franco M, Prade B and Mysyrowicz A 2001 *Opt. Commun.* **191** 333
- [13] Smelser C, Mihailov S and Grobncic D 2005 *Opt. Express* **13** 5377
- [14] Eaton S, Zhang H, Herman P, Yoshino F, Shah L, Bovatsek J and Arai A 2005 *Opt. Express* **13** 4708
- [15] Smelser C W, Grobncic D and Mihailov S J 2004 *Opt. Lett.* **29** 1730